13. Systematic Features of Mass Yield Curves in Low-energy Fission of Actinides

Yuichiro NAGAME
Advanced Science Research Center, Japan Atomic Energy Research Institute
Tokai-mura, Ibaraki 319-1195, Japan
e-mail: nagame@popsvr.tokai.jaeri.go.jp

Abstract

Characteristics of mass yield curves in fission of wide range of nuclides from pre-actinides through transactinides are reviewed and the following points are discussed. (1) Systematic trends of the mass yield distributions in low-energy proton-induced fission of actinides and in spontaneous fission of actinides are discussed in terms of weighted mean mass numbers of the light and heavy asymmetric mass yield peaks and widths of the heavy asymmetric mass yields. (2) Gross features of the two kinds of mass yield curves, symmetric and asymmetric ones, as a function of a fissioning nucleus. (3) Competition between the symmetric and asymmetric fission as a function of not only Z (proton number) but also N (neutron number) of a fissioning nucleus. (4) Experimental verification of the existence of two kinds of deformation paths in low energy fission of actinides; the first path is initiated at higher threshold energy and ends with elongated scission configuration, giving a final mass yield distribution centered around the symmetric mass division, "symmetric fission path". In the second path, a fissioning nucleus experiences lower threshold energy and results in more compact scission configuration, which gives a double humped mass distribution always centered around A=140 for the heavier fragment, "asymmetric fission path". (5) Interpretation of the "bimodal fission" observed in the spontaneous fission of heavy actinides as the presence of the two fission paths of the ordinary asymmetric one and a strongly shell-affected symmetric path from the systematic analysis of scission configurations. (6) A dynamical fission process deduced from the analysis of the experimental mass yield curves and the correlation data of neutron multiplicity and fragment mass and total kinetic energy. (7) Prediction of the characteristics of gross properties of fission in superheavy nuclei around $^{280}114$. (8) Characteristics of highly asymmetric fission: formation cross section as a function of excitation energy and angular distribution. (9) Based on the systematic analysis of the heavy asymmetric mass yield curves in thermal neutron- and proton-induced fission of actinides, and spontaneous fission of medium and heavy actinides, the relation between the fragment shell structure and the shape of the mass yield curves which reflect the final mass division process is discussed.

D.C. Hoffman & M.M. Hoffman, Ann. Rev. Nucl. Sci. 24, 151(1974)

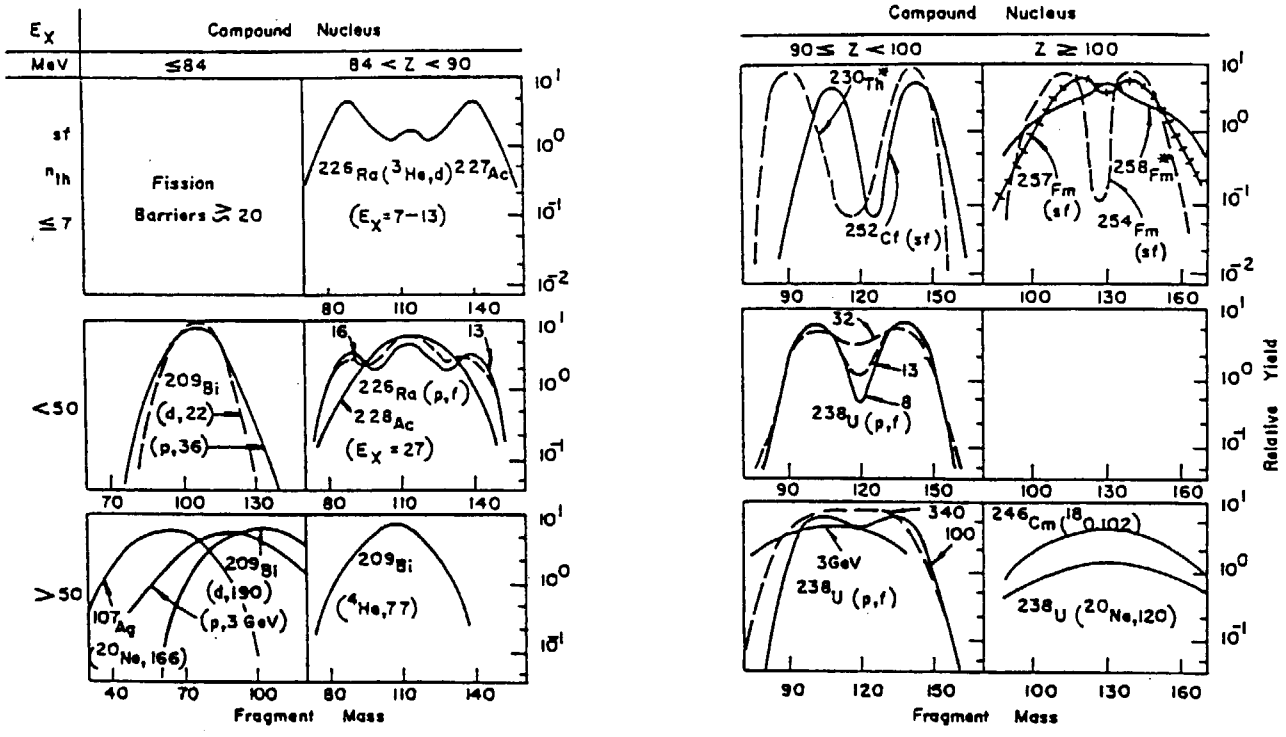

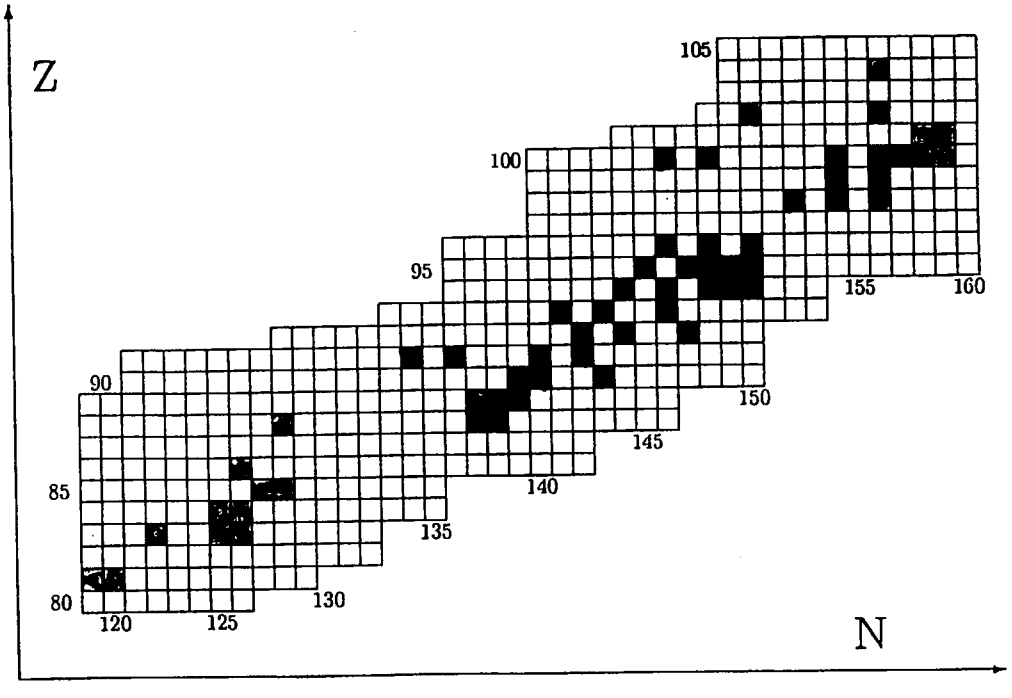

●: symmetric
●: symmetric & asymmetric
●: asymmetric

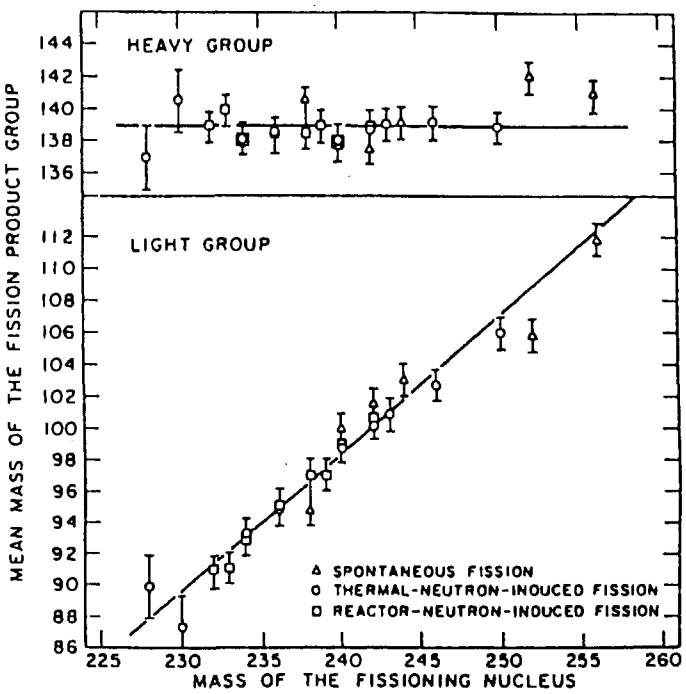

Figure 4 Average masses of light and heavy groups as a function of the mass of the fissioning nucleus (26).

K.F. Flyn et al. P.R.C 5. 1725(1972).

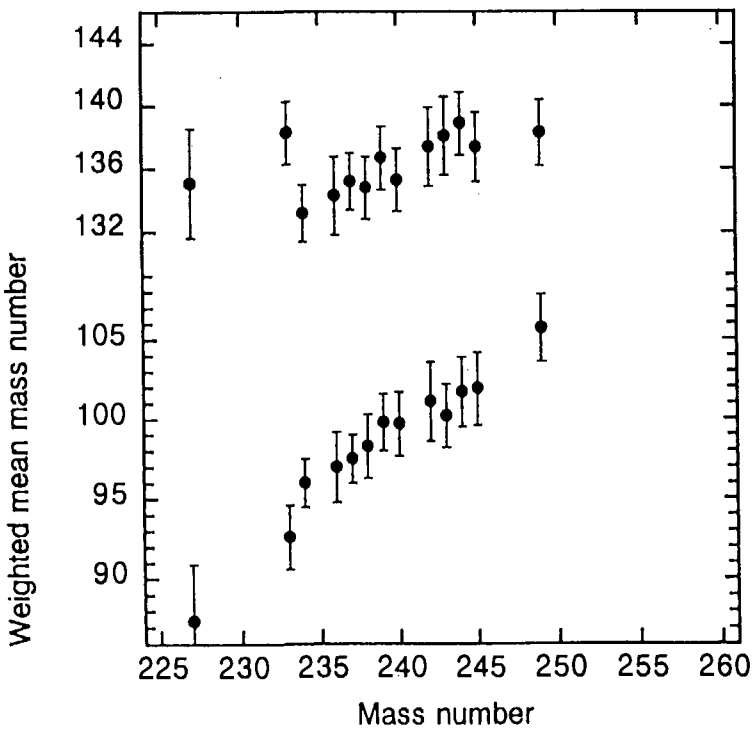

Z. Qin et al. Radiochim. Acta(in press).

$p + {}^{248}Cm$

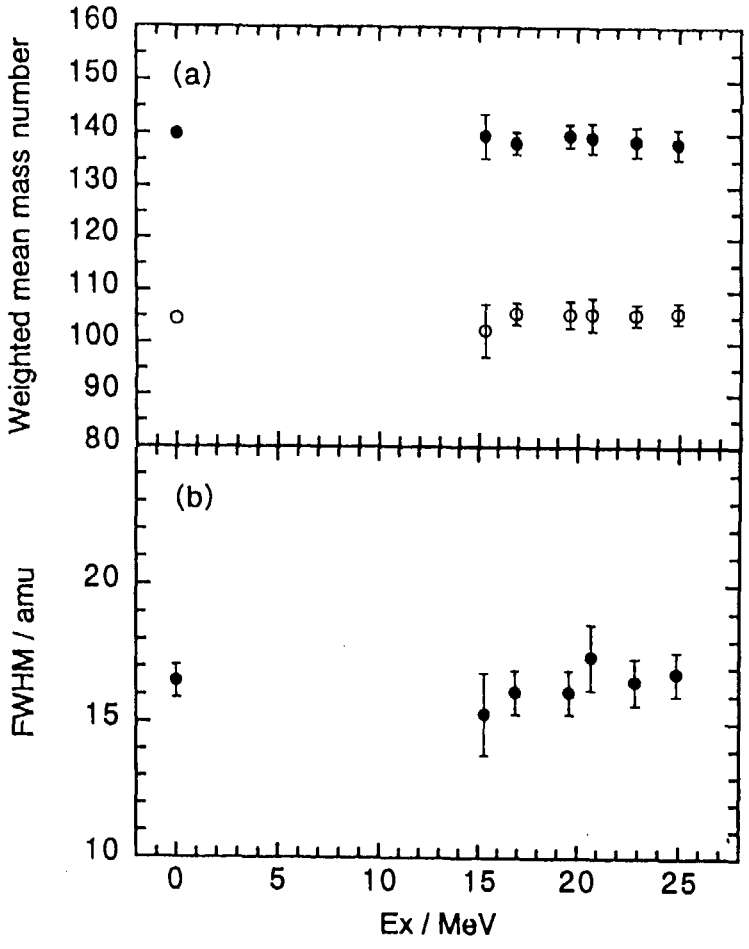

$^{248}Cm(SF)$

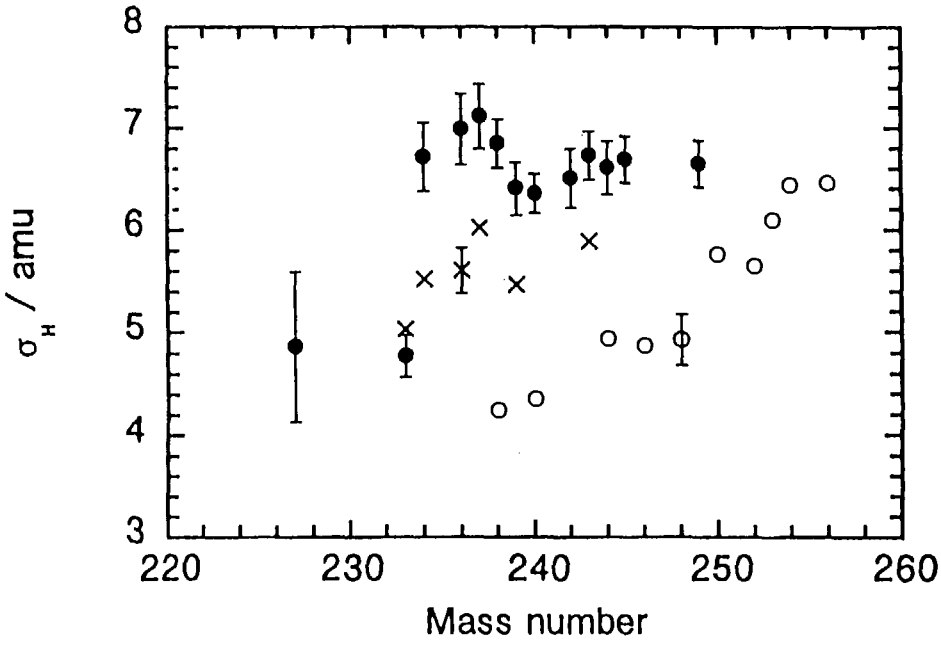

M.R. Lane, P.R.C 53, 2893(1996)

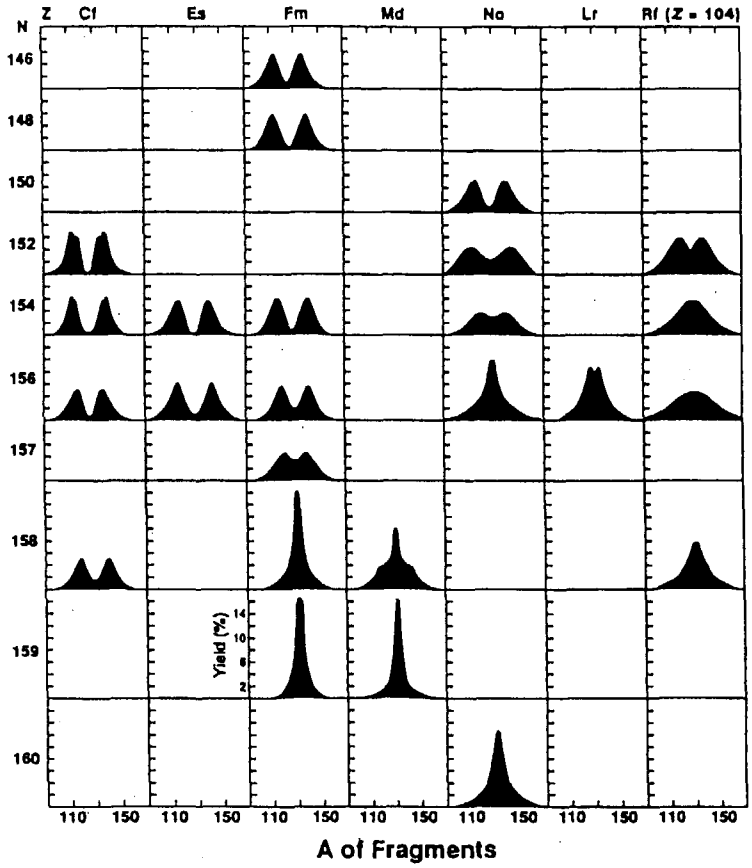

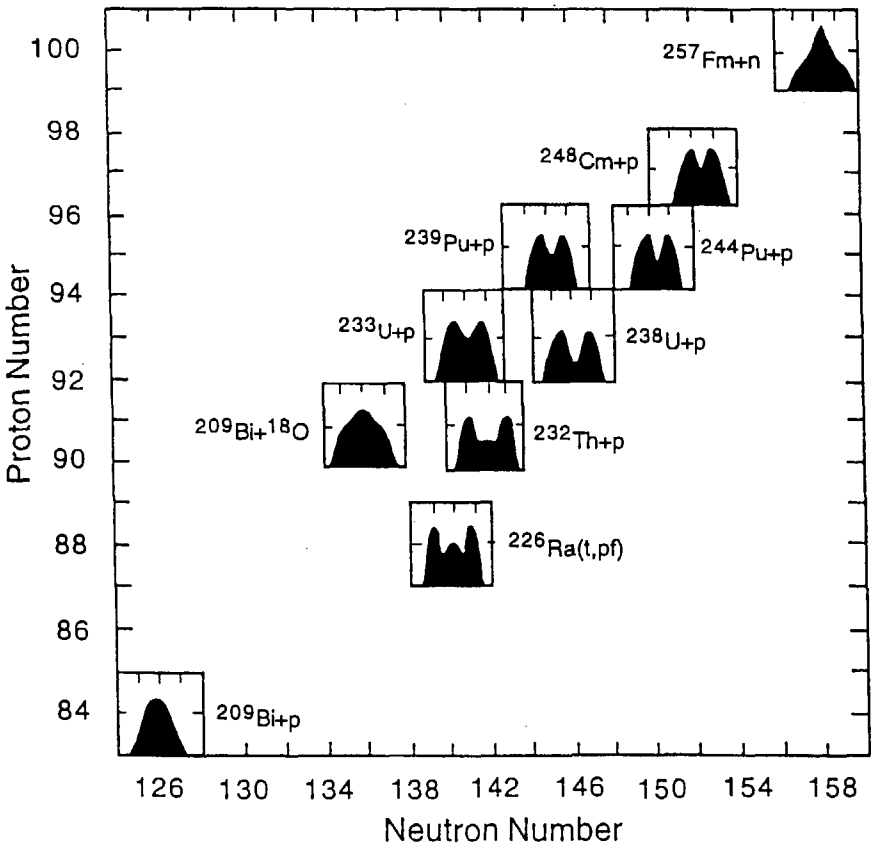

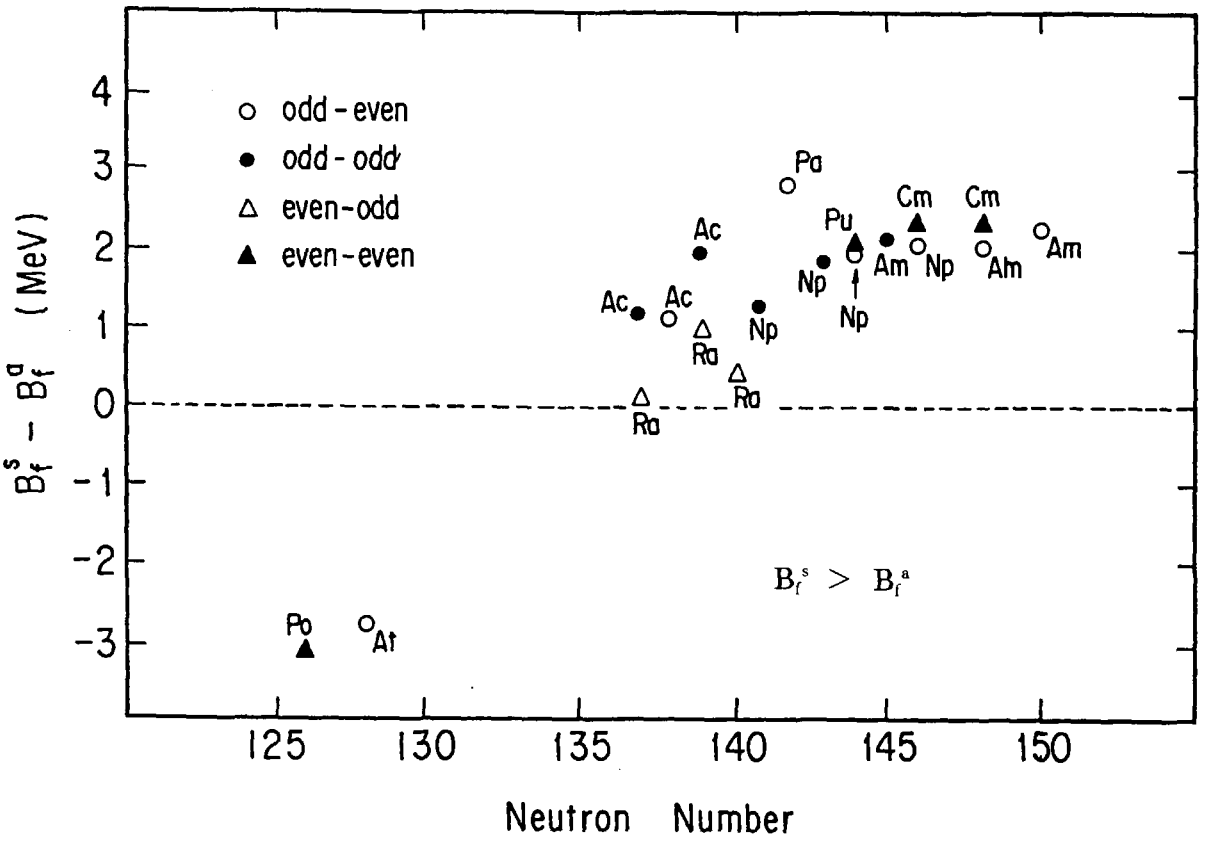

K.-H. Schmidt et al. / Nuclear Physics A630 (1998) 208c–214c

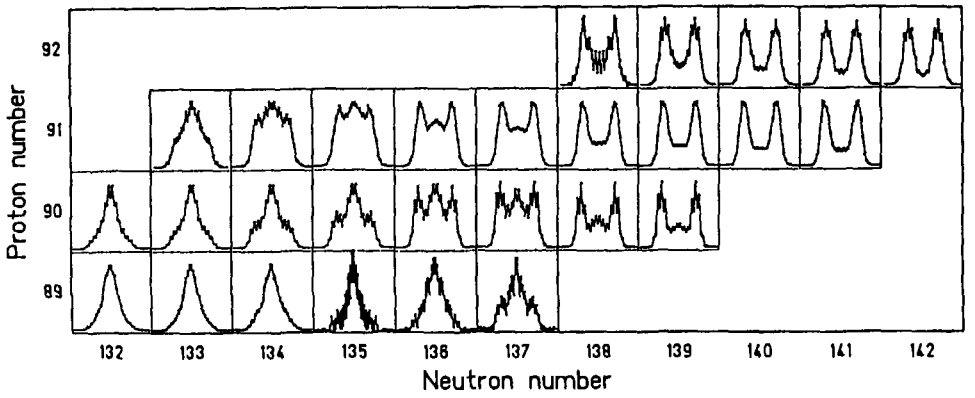

15 MeV p + ^{232}Th, ^{238}U, ^{244}Pu, ^{248}Cm

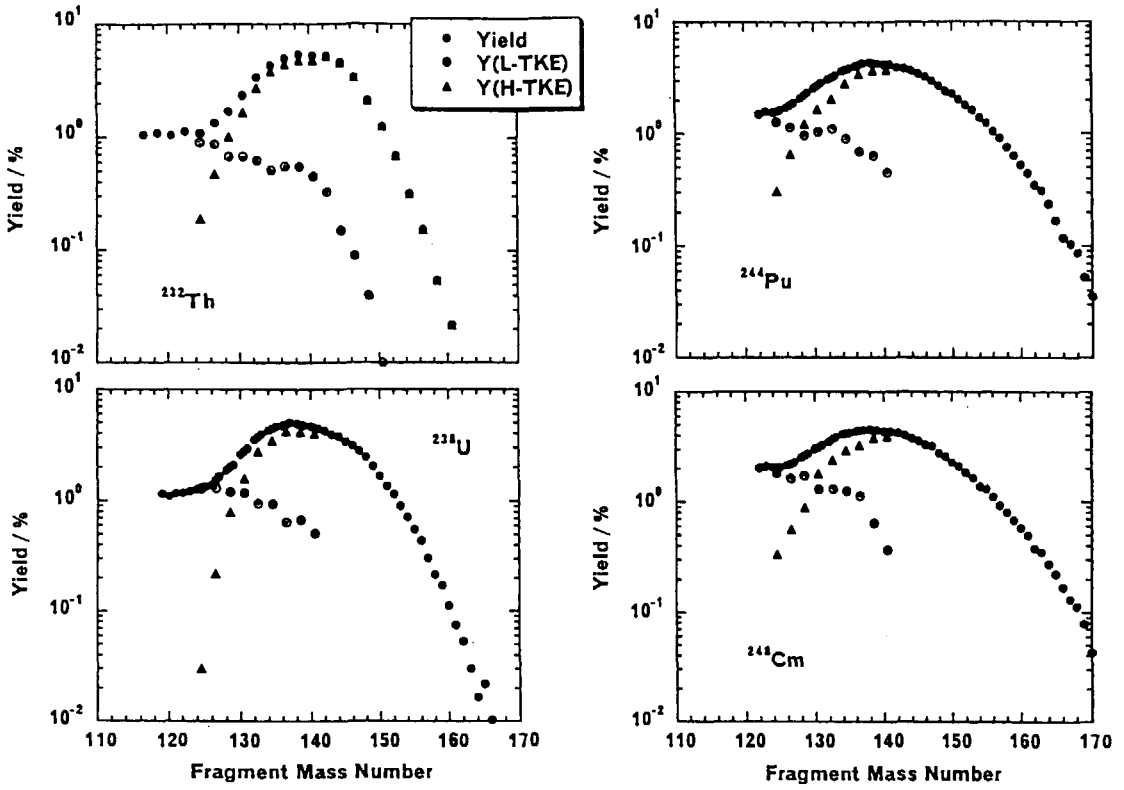

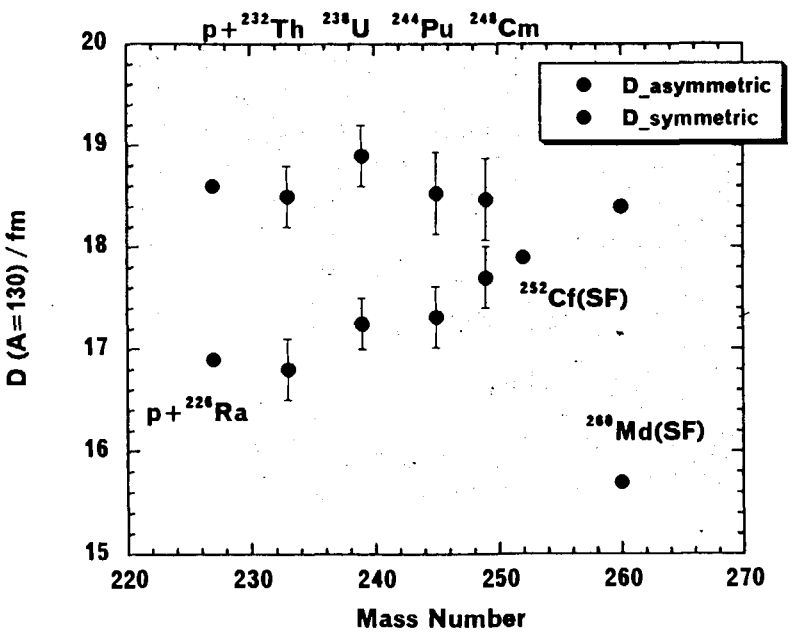

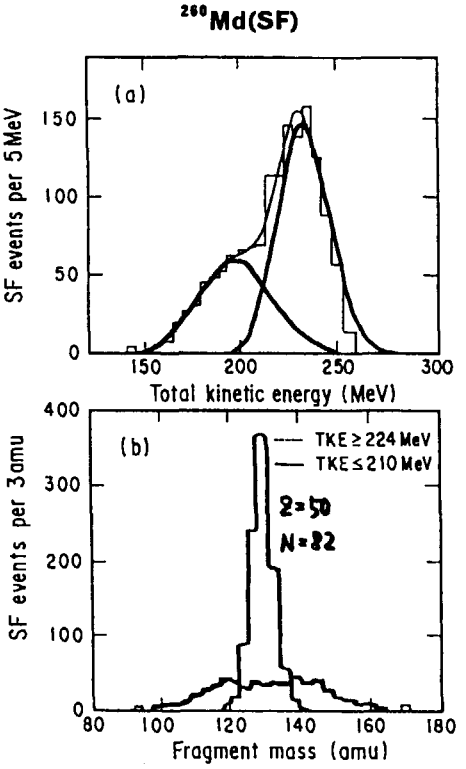

p + ^{226}Ra : E. Konechny and H.W. Schmitt, Phys. Rev. 172, 1213 (1968).
^{252}Cf(SF) : Yu.A. Barashkov et al., Sov. J. Nucl. Phys. 13, 668 (1971).
^{260}Md(SF) : J.F. Wild et al., Phys. Rev. C 41, 640 (1990).

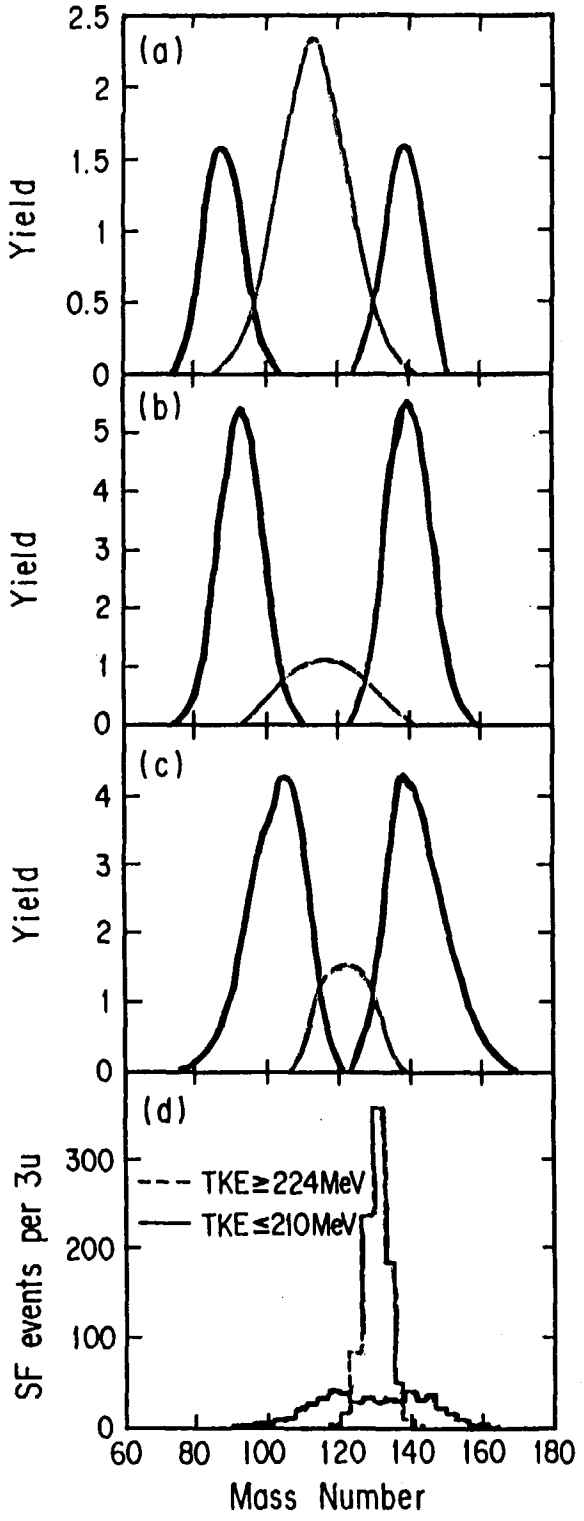

13 MeV p + ^{226}Ra

15 MeV p + ^{232}Th

15 MeV p + ^{244}Pu

^{260}Md(SF)

Correlation between final mass division and fragment shell structure

The heavier wing of the heavy asymmetric yield curve becomes broad with A_H, while the lighter wing of that constitutes the steep cliff around the mass region A=130.

CN	^{233}Pa	^{239}Np	^{245}Am	^{249}Bk
N/Z	1.56	1.57	1.58	1.57
A_L(N=50)	82	82	82	82
A_H	151	157	163	167

Heavy fragment shell structure with A=132 (Z=50, N=82)

Effect of the complementary light fragment with N=50

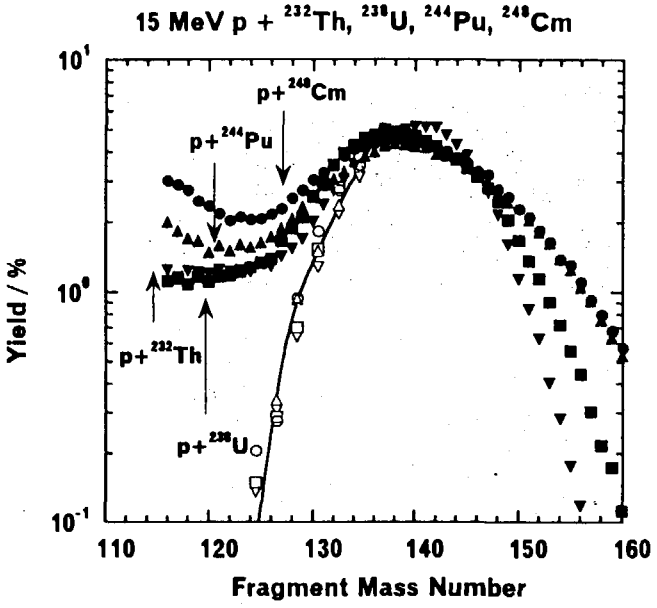

Radiochim. Acta 76. 173(1997).

K. Tsukada *et al.*

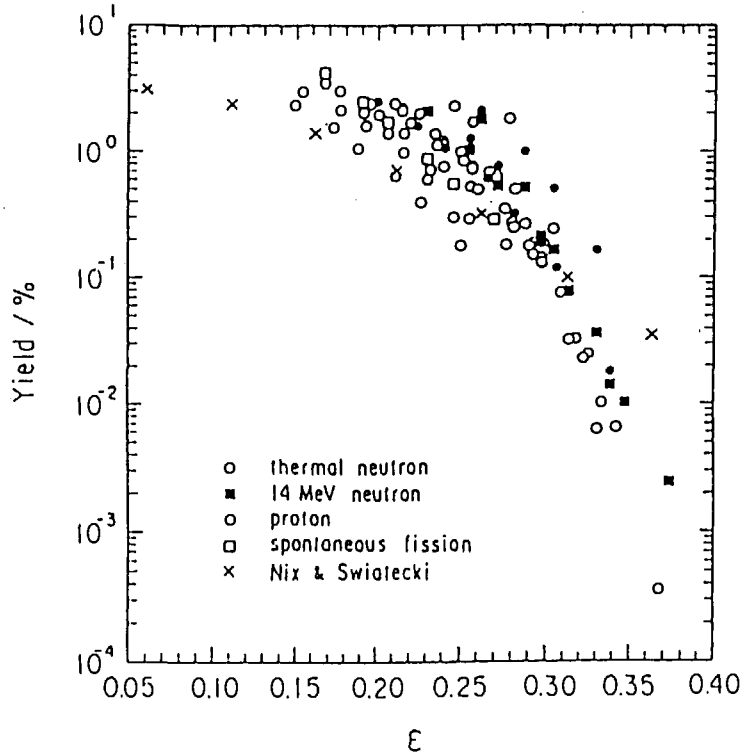

$$\frac{W(180^\circ)}{W(90^\circ)} = 1 + \frac{\langle I^2 \rangle}{4K_e^2} \qquad \kappa_e^2 = \frac{\beta_{eff} \cdot T_{saddle}}{\hbar^2}$$

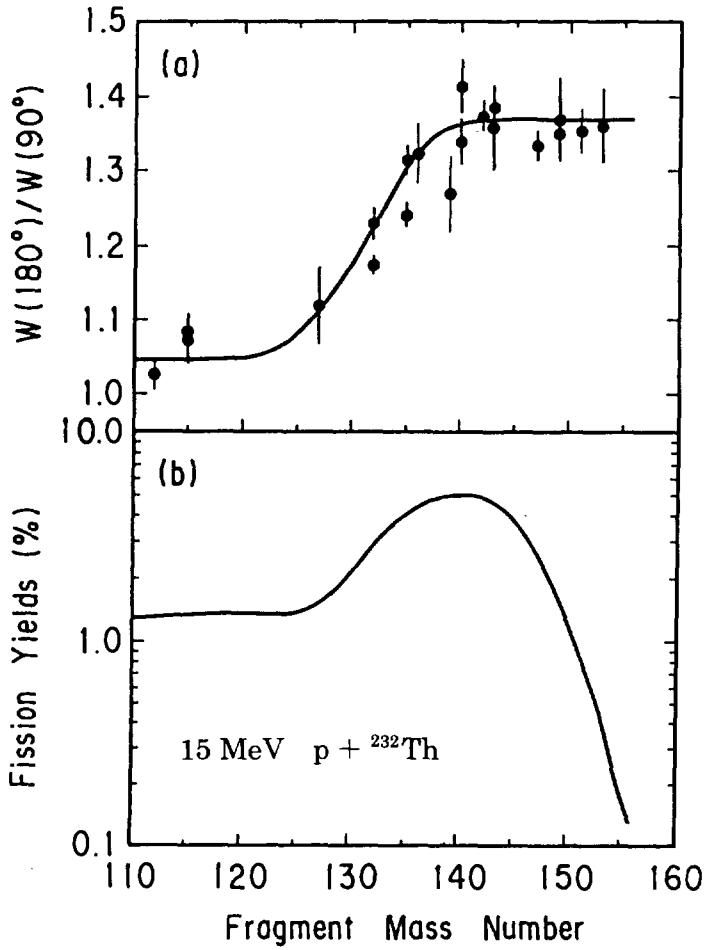

15 MeV p + ^{244}Pu

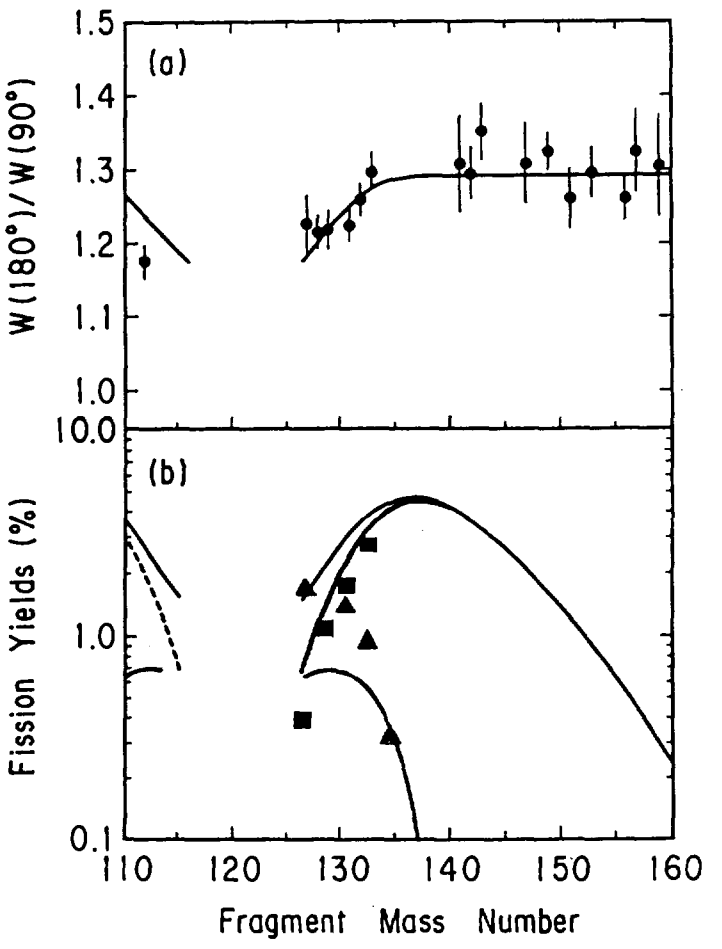

References

[1] Hoffman D.C. and Hoffman M.M.: Ann. Rev. Nucl. Sci. **24**, 151 (1974).

[2] Flyn K.F. *et al.*: Phys. Rev. C **5**, 1725 (1972).

[3] Qin Z. *et al.*: Radiochim. Acta (in press).

[4] Lane M.R. *et al.*: Phys. Rev. C **53**, 2893 (1996).

[5] Ohtsuki T. *et al.*: Phys. Rev. C **48**, 1667 (1993).

[6] Nishinaka I. *et al.*: Phys. Rev. C **56**, 891 (1997).

[7] Schmidt K.-H. *et al.*: Nucl. Phys. **A630**, 208c (1998).

[8] Nagame Y. *et al.*: Phys. Lett. B **387**, 26 (1996), J. Radioanal. Nucl. Chem. **239**, 97 (1999).

[9] Zhao Y.L. *et al.*: J. Radioanal. Nucl. Chem. **239**, 113 (1999), Phys. Rev. Lett. (in press).

[10] Zhao Y.L.: Ph. D. Thesis, Tokyo Metropolitan University (1999).

[11] Tsukada K. *et al.*: Radiochim. Acta **76**, 173 (1997).

[12] Tsukada K. *et al.*: Eur. Phys. J. A **2**, 153 (1998).